Isotope Effect for Plasma Detachment in Helium and Hydrogen/Deuterium Mixture Plasmas*)

Xinyue GUO, Hirohiko TANAKA, Shin KAJITA[1)], Noriyasu OHNO, Shogo HATTORI and Keiji SAWADA[2)]

Graduate School of Engineering, Nagoya University, Nagoya 464-8603, Japan
[1)]Institute of Materials and Systems for Sustainability, Nagoya University, Nagoya 464-8603, Japan
[2)]Graduate School of Engineering, Shinshu University, 4-17-1 Wakasato, Nagano 380-8553, Japan

(Received 6 January 2022 / Accepted 24 February 2022)

To investigate the isotope effect on the plasma detachment in helium (He) and hydrogen (H)/deuterium (D) mixture plasmas, we performed H_2, D_2 or He gas puffing into He plasma in the linear plasma device NAGDIS-II. Axial distributions of electron density (n_e) and electron temperature (T_e) were obtained using a movable Langmuir probe. Additionally, optical emission spectroscopy (OES) was applied to measure axial distributions of Balmer lines and He I lines. When the neutral gas pressure was high ($\Delta P_n = 7 \sim 10$ mTorr), n_e distribution in He-D_2 mixture plasma was similar to that in pure He plasma, showing a sharp decrease at the downstream region where $T_e < 1$ eV. In contrast, in He-H_2 mixture plasma, a decrease in n_e was confirmed from upstream region where $T_e > 1$ eV. The upstream H_α/H_γ in He-H_2 plasma was significantly larger than the D_α/D_γ in He-D_2 plasma at the same T_e. This result indicated that molecular activated recombination (MAR) processes significantly occurred in He-H_2 plasma, while electron-ion recombination (EIR) processes were dominant in He-D_2 and pure He plasmas.

Keywords: detached helium plasma, hydrogen/deuterium puffing, isotope effect, molecular activated recombination, electron-ion recombination

DOI: 10.1585/pfr.17.2402027

1. Introduction

In magnetic confinement fusion devices, an isotope effect is well-known to affect core and edge plasma characteristics [1–7]. In divertor region, plasma detachment is thought to be a promising method to reduce the divertor heat load, and the molecular activated recombination (MAR) processes were reported to have a dependence on isotope species, e.g., the reaction rates of MAR for hydrogen (H) and deuterium (D) plasmas are different [8]. Furthermore, in the actual fusion reactor condition, there is also helium (He) in addition to H and D. Therefore, it is required to clarify the isotope effect for plasma detachment in hydrogen isotopes and He mixture plasmas.

To investigate detailed atomic and molecular processes like MAR, usage of linear plasma devices has an advantage because of their abundant diagnostic systems, controllability, and reproducibility. In the linear divertor plasma simulator NAGDIS-II, previous research clearly revealed that MAR processes dominantly occurred in the He-H_2 mixture plasma, while electron-ion recombination (EIR) processes are dominant in the pure He plasma [9].

In this study, we first compared spatial distributions of plasma parameters and line emissions in He-H_2, He-D_2, and pure He plasmas along the magnetic field in NAGDIS-II. To measure electron density, n_e, and electron temperature, T_e, along the axis, a movable Langmuir probe was employed. In addition, line emissions were obtained by using a spectrometer. The degree of plasma detachment was controlled by adjusting the H_2, D_2, or He gas puffing rate from the downstream.

2. Experiment Setup

Experiments were conducted in the linear divertor plasma simulator NAGDIS-II. A schematic of experiments is shown in Fig. 1. At first, we generated a pure He plasma without any additional gas puffing from the downstream. The discharge current and the magnetic field strength were 100 A and 0.2 T, respectively. At that time, base He neutral pressure, P_{n0}, was measured as 6.5 mTorr at the middle position of the vacuum vessel by using a capacitance gauge (ANELVA, M-342DG-1D). Further, we injected secondary gas (H_2 or D_2 or He) from downstream at several different flow rates, and measured the total gas pressure, P_n, in the same way. By using P_n, the partial (additional) pressure was calculated as $\Delta P_n = P_n - P_{n0}$.

To obtain plasma parameters of n_e and T_e, double probe measurement was done with the two-dimensional (2D) movable Langmuir probe system [10], which demonstrated accurate measurements of low-temperature detached helium plasmas [11]. By moving the probe position, axial distributions of n_e and T_e at $1.36\,\mathrm{m} < x < 2.02\,\mathrm{m}$

Corresponding author's e-mail: h-tanaka@ees.nagoya-u.ac.jp
*) This article is based on the presentation at the 30th International Toki Conference on Plasma and Fusion Research (ITC30).

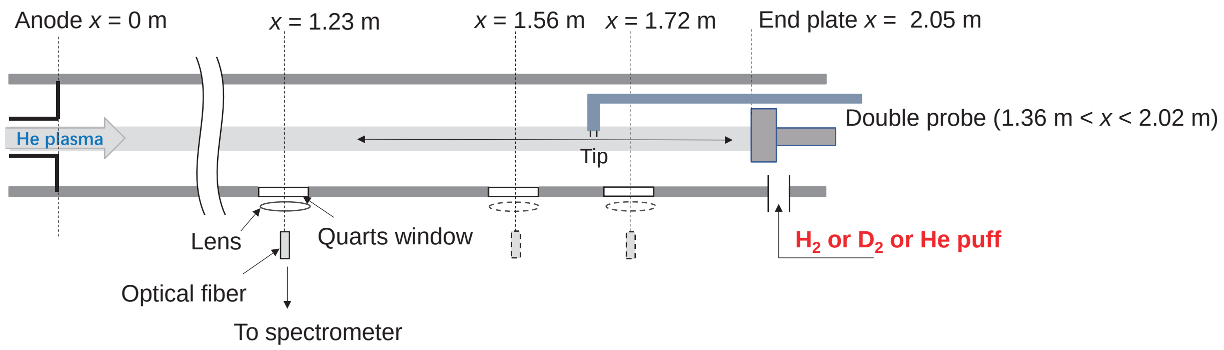

Fig. 1 Schematic of experimental setup in NAGDIS-II.

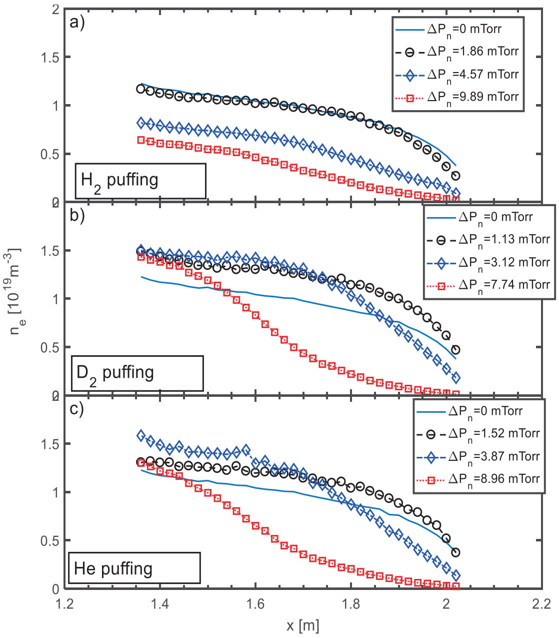

Fig. 2 Axial distributions of n_e in (a) H_2 puffing case, (b) D_2 puffing case, and (c) He puffing case.

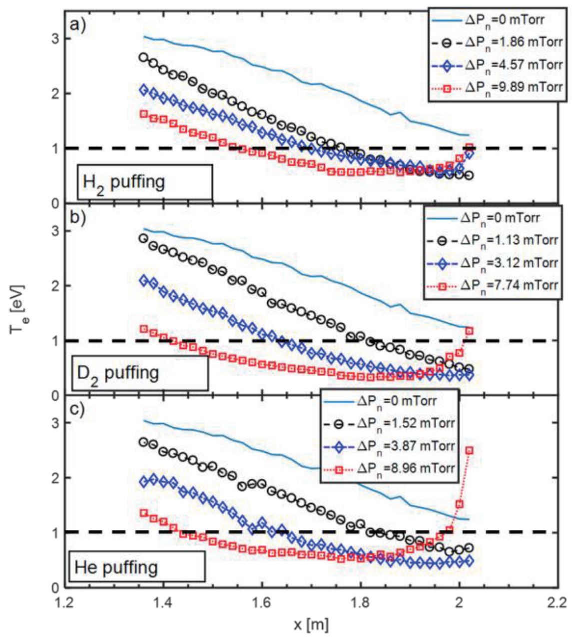

Fig. 3 Axial distributions of T_e in (a) H_2 puffing case, (b) D_2 puffing case, and (c) He puffing case.

were obtained, where x is the distance from the anode. In addition, to understand atomic and molecular processes, spectroscopic measurement was also done at three axial positions of $x = 1.23$ m, 1.56 m and 1.72 m with a spectrometer (SPEX 750 M). Intensities were calibrated by using an integrating sphere.

3. Double Probe and Spectroscopic Measurements

3.1 Axial distribution of electron density

Figures 2 (a), (b), and (c) show axial distributions of n_e when H_2, D_2, or He gas was injected into He plasmas, respectively. The left-hand side (smaller-x side) corresponds to the upstream direction in the device. Noted that n_e was deduced by assuming that the ion mass was the same with that of the He ion. Therefore, in H_2 or D_2 puffing case, obtained n_e would be overestimated up to 2 or ~1.4 times, respectively. Further, solid line ($\Delta P_n = 0$) in each figure indicates the pure He plasma parameter.

In Fig. 2, it is clearly seen that n_e distributions of D_2 and He puffing cases are similar, in which a sharp decrease in n_e is observed in the measurement range when ΔP_n is high. In contrast, in the H_2 puffing case, such a sharp axial reduction is not found in the measurement range, while n_e at the upstream region ($x \sim 1.4$ m) decreases with an increase of ΔP_n. The decrease in the upstream density in the H_2 puffing case is consistent with previous researches [9, 12].

3.2 Axial distribution of electron temperature

Figures 3 (a), (b), and (c) show axial distributions of T_e when H_2, D_2, or He was injected into He plasmas, respectively. It is noted that T_e in front of the end plate

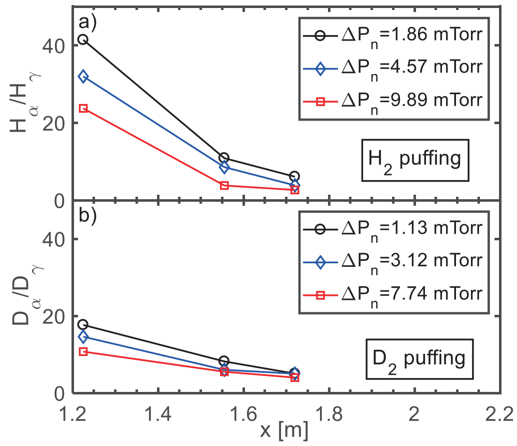

Fig. 4 4 Axial distributions of (a) H_α/H_γ in the H_2 puffing case and (b) D_α/D_γ in the D_2 puffing case.

($x \sim 2$ m) is unreliable because of too-small n_e and disturbance from the end plate.

By comparing n_e in Fig. 2 (c) and T_e in Fig. 3 (c) in the He puffing case, it can be confirmed that n_e begins to decrease sharply when T_e drops to below 1 eV, which is due to the three-body recombination in EIR processes. In addition, T_e distributions in D_2 puffing case are similar to those in He puffing case. Considering the result that n_e distributions in D_2 and He puffing cases are also similar, EIR processes would be also dominant in He-D_2 mixture plasma. In contrast, in the upstream region ($x \sim 1.4$ m) in H_2 puffing case, where n_e decreases with high ΔP_n, T_e is found to be over 1 eV. This result indicates that MAR processes, which can occur when $T_e > 1$ eV, are dominant in He-H_2 mixture plasma.

3.3 Intensity ratio of Balmer lines

In addition to the double probe measurement, we collected spectroscopic signals. Figure 4 shows axial distributions of H_α/H_γ in the H_2 puffing case and D_α/D_γ in the D_2 puffing case. We found that the obtained range of H_α/H_γ is about 20 - 40 in the upstream region, which is significantly larger than D_α/D_γ (< 20). Generally, MAR processes produce neutrals in low excited states (n = 3, 4) while EIR produces highly-excited-state neutrals [12]. Therefore, the difference between H_2 and D_2 puffing cases can be explained by considering that MAR is dominant in the upstream region of the He-H_2 mixture plasma and EIR is dominant in the He-D_2 mixture plasma.

In the downstream region in the H_2 puffing case, H_α/H_γ becomes comparable to that in the D_2 puffing case. As shown in Fig. 3 (a), T_e decreases in the axial direction, and particularly for ΔP_n = 9.89 mTorr, T_e is found to be below 1 eV at $x > 1.55$ m. Therefore, it is considered that the three-body recombination in EIR processes occurs in the downstream region also in the H_2 puffing case. This three-body recombination increases the population density of the highly excited level neutrals, which reduces the ratio of H_α/H_γ.

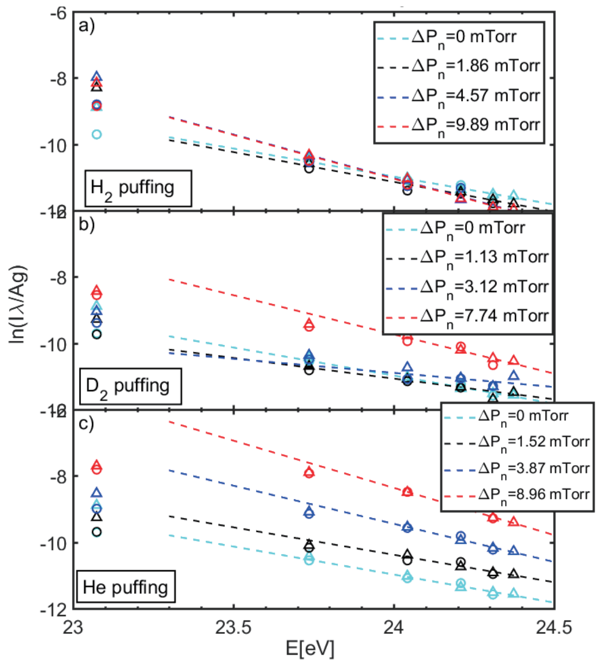

Fig. 5 Boltzmann plots in (a) H_2 puffing case, (b) D_2 puffing case, and (c) He puffing case at x = 1.23 m. Triangles and circles represent intensities of triplet (D→P $n = 3 \sim 8 \rightarrow 2$) and singlet (D→P $n = 3 \sim 7 \rightarrow 2$) states, respectively. The dotted lines were fitted ones by a linear function with intensities from triplet states of $n = 5 \sim 8$ and singlet states of $n = 5 \sim 7$.

3.4 Intensity of He I lines

Figure 5 shows Boltzmann plots of He I lines in the upstream region in H_2, D_2, and He puffing cases based on the following equation:

$$\ln\left(\frac{I_{pq}\lambda_{pq}}{A_{pq}g_p}\right) = -\frac{E_p}{k_B T_{exc}} + C,$$

where I_{pq} is the emission line intensity from level p to level q, λ_{pq} is the wavelength, A_{pq} is the spontaneous emission probability, g_p is the statistical weight, E_p is the potential energy, k_B is the Boltzmann constant, T_{exc} is excitation temperature, and C is a constant. The horizontal axis and vertical axis in Fig. 5 are E_p and $\ln(I_{pq}\lambda_{pq}/A_{pq}g_p)$, respectively.

In this figure, triangles and circles represent intensities of triplet (D→P $n = 3 \sim 8 \rightarrow 2$) and singlet (D→P $n = 3 \sim 7 \rightarrow 2$) states, respectively. Here, the singlet state of $n = 8 \rightarrow 2$ is not used because the intensity was too weak. The dotted lines were fitted ones by a linear function with intensities from triplet states of $n = 5 \sim 8$ and singlet states of $n = 5 \sim 7$. It is seen that when ΔP_n is high in He and D_2 puffing cases (especially with red markers), intensities from n = 3 are smaller than fitted lines. In contrast, in H_2 puffing case, the intensity from n = 3 is higher than the fitted line.

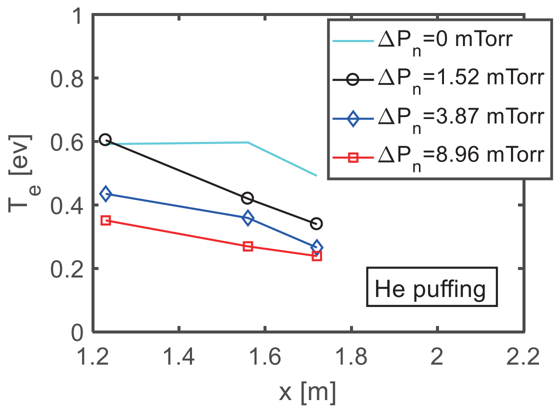

Fig. 6 Axial distributions of T_e estimated with Boltzmann method in the He puffing case.

In the He puffing (pure He) case, T_e was estimated with the Boltzmann method by assuming $T_e \sim T_{exe}$, as shown in Fig. 6. By comparing Fig. 3 (c), deduced T_e are much smaller than T_e measured by the double probe. The smaller T_e, which are below 1 eV in all cases and positions, would be attributed to the line emissions from the low-T_e plasma in the peripheral region. Similarly, intensities of hydrogen and deuterium emission lines may also be affected by the surrounding plasma. For further detailed analysis, spatially resolved emission measurement by using the Abel transform or the tomographic technique would be needed.

4. Discussion

It was found that MAR processes would be dominant in the upstream region of the He-H_2 mixture plasma from following results: (i) n_e decreases despite $T_e > 1$ eV and (ii) densities of low-excited-state hydrogen neutrals are relatively high. In particular, result (ii) indicates that the dissociative recombination of HeH^+ would be an important process. In contrast, in the He-D_2 mixture plasma, parameter distributions resemble those in the pure He plasma and sharp reduction of n_e is seen at $T_e < 1$ eV, which indicates that the three-body recombination process would be dominant in the EIR processes.

One of the reasons for the difference in the MAR between H_2 and D_2 puffing cases is the difference of the cross section (σ) of following reactions:

$$He^+ + H_2 \rightarrow HeH^+ + H, \tag{1}$$

$$He^+ + D_2 \rightarrow HeD^+ + D. \tag{2}$$

In Ref. [13], when the kinetic energy (E) is less than ~7 eV, σ of reaction (1) (σ_{reac1}) is larger than that of reaction (2) (σ_{reac2}). Particularly, when E <~4 eV, σ_{reac2} becomes significantly small. Therefore, it is thought that a lot of HeH^+ was generated and then the dissociative recombination occurred in the He-H_2 mixture plasma.

In Fig. 4, it was stated that MAR strongly occurs in upstream because H_α/H_γ was larger. However, a more careful discussion is needed because the axial distribution of T_e is different in H_2 and D_2 puffing cases, as shown in Fig. 3. The observed population intensities are influenced by not only MAR but also electron impact excitation. At ΔP_n = 1.86 mTorr in H_2 puffing and ΔP_n = 1.13 mTorr in D_2 puffing cases, although the upstream T_e would be the almost same (~3 eV), H_α/H_γ (~40) is much larger than D_α/D_γ (~20) at x = 1.23 m. This result indicates that MAR is dominating in H_2 gas puffing.

Figure 5 shows intensities of He Balmer series from $n = 3$ to $n = 8$. The population density at $n = 3$ becomes large with H_2 gas puffing in He-H_2 plasma. A similar phenomenon has been observed in previous studies and analyzed by the collisional radiation code CRAMD [9]. However, the formation of He atoms with low excitation levels in the dissociative recombination process of HeH^+ has not yet been established theoretically, and further studies are needed.

5. Conclusion

We investigated isotope effects for plasma detachment in He-H_2/D_2 mixture plasmas in linear plasma device NAGDIS-II by using a movable double probe and a spectrometer. Obtained results suggest that the MAR process with HeH^+ generation dominantly occurred in the He-H_2 mixture plasma. On the other hand, MAR is not dominant while EIR processes occurred in the He-D_2 mixture plasma like in the pure He plasma.

In an actual fusion reactor, D and tritium (T) are used. Therefore, it is important to consider about molecular processes regarding HeT^+. In this study, we performed spectroscopic measurement just at three axial positions. In the future, we are planning to measure wide and continuous distributions of the light emission in axial and radial directions, by installing an optical fiber to the 2D movable probe. By applying the Abel transform or the tomographic technique, spatially resolved analyses will be done. Furthermore, in this study, the ratio of the He partial pressure to the total pressure was a minimum of ~40% and a maximum of 100%. This ratio is much higher than that in the fusion reactor (~5%). Therefore, it would be important to investigate the effect of a smaller amount of He on the formation of the hydrogen-isotope detached plasma.

Acknowledgements

This work was supported by JSPS KAKENHI (18KK0410, 19K03802, 20H00138), NIFS Collaboration Research program (NIFS19HDAF003, NIFS19KLPP060, NIFS20KUGM149), the Nitto Foundation, and NINS program of Promoting Research by Networking among Institutions (01411702).

[1] M. Bessenrodt-Weberpals *et al.*, Nucl. Fusion **33**, 1205

(1993).
[2] C.F. Maggi *et al.*, Plasma Phys. Control. Fusion **60**, 014045 (2018).
[3] H. Takahashi *et al.*, Nucl. Fusion **58**, 106028 (2018).
[4] B. Sieglin *et al.*, Plasma Phys. Control. Fusion **58**, 055015 (2016).
[5] H. Tanaka *et al.*, Nucl. Mater. Energy **19**, 378 (2019).
[6] M. Osakabe *et al.*, Nucl. Fusion **62**, 042019 (2022).
[7] M. Kobayashi *et al.*, Nucl. Fusion **62**, 056006 (2022).
[8] A.S. Kukushkin *et al.*, Nucl. Mater. Energy **12**, 984 (2017).
[9] N. Ohno *et al.*, Phys. Rev. Lett. **81**, 818 (1998).
[10] N. Ohno *et al.*, Nucl. Mater. Energy **19**, 458 (2019).
[11] Y. Hayashi *et al.*, Contrib. Plasma Phys. **59**, e201800088 (2019).
[12] D. Nishijima *et al.*, Plasma Phys. Control. Fusion **44**, 597 (2002).
[13] R.K. Janev, *Atomic and Molecular Processes in Fusion Edge Plasmas* (Plenum Press · New York and London 13350).